Available online at www.sciencedirect.com
ScienceDirect
Polymer 47 (2006) 6362–6378
polymer
www.elsevier.com/locate/polymer

Influence of composition and annealing on the structure development in biaxially stretched PEN/PEI/PEEK ternary blends

Xixian Zhou[1], M. Cakmak*

Institute of Polymer Engineering, The University of Akron, Akron, OH 44325-0301, USA

Received 17 May 2006; received in revised form 30 June 2006; accepted 3 July 2006
Available online 25 July 2006

Abstract

The effect of biaxial stretching and annealing on the structure development in ternary blends of PEN/PEI/PEEK on mostly PEN-rich compositions has been investigated. Both PEN and PEEK are melt miscible with PEI. The addition of PEI greatly suppresses the crystallizability of the PEN while enhancing the glass transition temperature. The addition of PEEK to high PEI containing PEN/PEI recovers this crystallizability with the end result being the high T_g materials that can strain harden. The crystallization habit is mostly PEN at PEN-rich corner of the ternary diagram. The increase of PEI concentration beyond 20% eliminates the crystallizability of PEN and addition of as little as 10% PEEK causes these blends to crystallize upon stretching in the rubbery state.

Keywords: Ternary blends; Biaxial stretching; PEN/PEI/PEEK

1. Introduction

Poly(ethylene 2,6-naphthalene dicarboxylate) (PEN) is a semi-crystalline aromatic polycondensate having the following repeat unit.

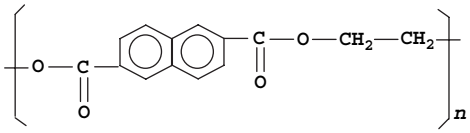

PEN exhibits high mechanical, thermal, chemical and dielectric properties [1]. One of its most important characteristics is its resistance to permeation of small gas molecules, particularly, oxygen. This makes it a very attractive candidate for food packaging and beverage bottle applications [2]. Its high thermal stability and mechanical characteristics make it suitable for backing substrate in magnetic recording tapes [3–5] and tire cords [6].

PEN can be quenched into amorphous form or crystallized form by changing the thermal and/or stress history into two crystal structures. The first is called α modification (triclinic, $a = 0.651$ nm, $b = 0.575$ nm, $c = 1.32$ nm, $\alpha = 81.33°$, $\beta = 90°$ and $\gamma = 100°$) [7], obtained by crystallizing PEN from amorphous form or from the melt below 240 °C. The second crystal structure is called β modification (also triclinic, $a = 0.926$ nm, $b = 1.559$ nm, $c = 1.273$ nm, $\alpha = 121.6°$, $\beta = 95.57°$ and $\gamma = 122.52$ nm) obtained by crystallizing it above about 240 °C [8].

Uniaxial and biaxial film deformation studies [9–11] indicate that initially amorphous PEN exhibits necking behavior during deformation even when it is stretched above the glass transition temperature and the necking develops and propagates in the sample up to the onset of stress hardening. Stretching the films beyond the stress hardening point allows the film to become increasingly uniform. The crystal structure of the

* Corresponding author.
E-mail address: cakmak1@uakron.edu (M. Cakmak).
[1] Current address: Polymer Technology Center, Saint-Gobain Performance Plastics Corp., 150 Dey Road, Wayne, NJ 07470, USA.

0032-3861/$ - see front matter © 2006 Elsevier Ltd. All rights reserved.
doi:10.1016/j.polymer.2006.07.007

deformed and annealed film was packed into low temperature modification (α), and naphthalene planes preferentially orient parallel to the film's surface during biaxial deformation. Biaxially deformed films exhibit a bimodal chain orientation resembling a woven cross (cross-hatched) fabric construction but uniplanar axial texture was found in the case of free-width uniaxially deformed films.

The addition of up to 20% PEI to PEN was found to reduce the sharp necking phenomenon during uniaxial deformation between glass transition temperature and the cold crystallization temperature [12]. It occurs as a result of molecular level miscibility between PEN and PEI that causes disruption of the preferential alignment of the naphthalene ring planes parallel to the film's surface in the presence of bulk PEI chains. In contrast to the bimodal cross-hatched morphology observed in equally biaxially stretched PEN, in-plane isotropy is observed in PEN/PEI blends.

In the previous research [12] on blends of the PEN/PEI pair, it was found that the PEI concentration beyond 20% causes significant reduction in strain induced and thermal induced crystallizability while increasing the glass transition temperature. One of the objectives of this research was to increase the glass transition temperature while maintaining the strain hardening behavior. This latter requirement is very important if the polymer system were to succeed in traditional processing operations such as tenter frame processing or double bubble tubular film blowing.

Poly(ether ether ketone) (PEEK) exhibits strain induced crystallization upon stretching from amorphous precursors in the rubbery ($T_g < T_p < T_{cc}$) temperature range [13]. Its onset of strain hardening is quite low and it is also known to be miscible with PEI [14]. It is, however, not miscible with PEN [15,16]. When PEI is added to the immiscible PEN/PEEK system, below about 40% PEI the ternary PEN/PEI/PEEK blends separate into two phases namely PEN-rich and PEEK-rich, and above this concentration, PEI acts as a solvent for both PEN and PEEK and forms a miscible phase in their amorphous state. These ternary blends exhibit necking-free uniaxial deformation even below the onset of stress hardening.

In this study, we present our detailed structural studies on the effect of composition and processing conditions on the development of structure in biaxially stretched PEN/PEI/PEEK ternary blends in their miscible region.

2. Experimental

2.1. Materials and their thermal properties

Poly(ethylene 2,6-naphthalate) (PEN) used in this work was kindly provided by Eastman Chemical. Poly(ether imide) (PEI, ULTEM 1000) was received from GE. Poly(ether ether ketone) (PEEK, 381G) was obtained from ICI. As received homopolymer pellets were dried in a vacuum oven at 120–140 °C for at least 12 h to remove the moisture for the thermal analysis and blending process. Their weight, number and z average molecular weight are tabulated in Table 1.

Table 1
Molecular weights of PEN, PEI, PEEK

Materials	$\overline{M}_n$	$\overline{M}_w$	$\overline{M}_z$
PEN[a]	12,500	42,000	66,000
PEI[a]	16,750	40,350	67,350
PEEK	15,000	35,000	

[a] From Eastman Chemical.

2.2. Melt-blending

A JSW intermeshing co-rotating twin screw extruder was used to melt-blend PEN, PEEK, with PEI. The screw diameter is 30 mm and the length of the screw is 32.5D. The melt-blending was performed in two steps: first, PEI was blended with PEEK; and then PEN was blended with these PEI/PEEK binary blends. This procedure was followed to reduce the melt processing temperature of PEEK thereby reducing the possibility of degradation in PEN that occurs at elevated temperatures.

In the first step, as received PEI and PEEK pellets were dry-blended and placed in an oven and were dried at 120 °C for at least 24 h under vacuum. Twin screw extruder barrel temperatures were gradually increased from 265 to 370 °C along the barrel and 370 °C at the die. In order to minimize degradation, the feed section of the extruder was blanketed by argon gas. The extrudates were quenched in a water bath and pelletized.

In the second step, the vacuum dried PEI/PEEK blends were first dry-blended with pre-dried PEN pellets. Then the premixed ternary blends were melt-blended using the same JSW twin screw extruder. Melting temperatures in the pressure and metering zones were set to 320–355 °C depending on the concentration of the blend. In order to minimize the decomposition of PEN, the vents on the extruder were closed, and the feeder, the hopper and the extruder were blanketed with argon gas. Ternary compositions of the blends numbered from #1 to #11 were prepared as shown in a ternary diagram in Fig. 1. This ternary diagram was extensively studied by Bicakci and Cakmak [16,17]. In our study, we focus our attention to the blends in their miscible PEN-rich region to study the PEN effect and to PEI-rich region to study PEEK effect. The blends selected for this purpose were #1, #2, and #3 (PEI-rich), and #6, #9, and #11 (PEN-rich).

2.3. Melt-casting

Dried PEN/PEI/PEEK pellets were melt-cast using a Prodex 1″ single screw extruder equipped with an 8″ wide sheet casting die and a chill roll take up device. The temperature of the melt at the die was maintained at 335–355 °C depending on the concentration. The blends with higher PEEK content require higher melting temperature. The chill roll temperature was controlled at 70–80 °C depending on the composition using a water circulating temperature control unit. The thickness of the sheets was found to be about 400–500 μm. The melt-cast sheets were cut into 140 × 140 mm square shape for uni- and biaxial stretching.

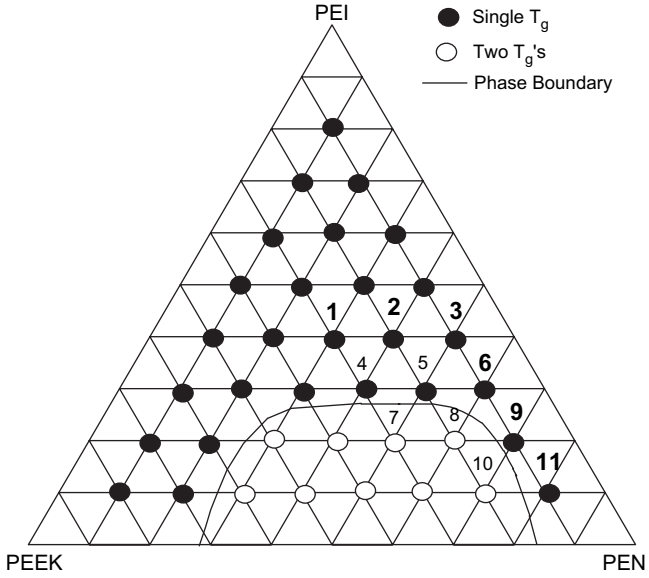

Composition (PEN/PEI/PEEK, wt%):

#1. 30/40/30;	#2. 40/40/20;	#3. 50/40/10;
#4. 40/30/30;	#5. 50/30/20;	#6. 60/30/10;
#7. 50/20/30;	#8. 60/20/20;	#9. 70/20/10;
#10. 70/10/20;	#11. 80/10/10	

Fig. 1. Ternary diagram of PEN/PEI/PEEK ternary blends.

2.4. Uni- and biaxial stretching

Biaxially oriented PEN/PEI/PEEK films with varying stretch ratios were produced using an Iwamoto biaxial stretcher (BIX-702). Three different stretching modes were used for all the blends: uniaxial constant width (UCW), unequal biaxial (UE), and equal biaxial (EB). Prior to stretching, the machine was heated to the desired stretching temperature for at least 3 h. The non-oriented sheet was mounted onto the pneumatic grips of the pre-heated machine and allowed for a 5 min thermal equilibrium time before the stretching. All samples were stretched at $T_g + 20$ °C (that was found to be optimum by previous uniaxial film stretching studies by Bicakci et al. [17,18]).

2.5. Annealing

Selected stretched films were cut to 80×80 mm and clamped in a square aluminum sandwich frame with dimensions 50×50 mm opening. They were then placed in a forced convection oven at 220 °C for 30 min. The oven was pre-heated for at least 4 h for thermal equilibrium before the samples were inserted.

2.6. Thermal analysis

2.6.1. Differential scanning calorimetry (DSC)

DSC thermal analysis of melt-cast PEN/PEI/PEEK blends, oriented and annealed films were performed on a Perkin Elmer DSC (DSC7) apparatus at a heating rate of 20 °C/min for all samples tested. The apparent crystallinity can be calculated using the following equations:

$$X(\%) = \frac{\Delta H_{\text{exp}}}{\Delta H^{\text{o}}} \times 100 \tag{1}$$

$$\Delta H_{\text{exp}} = \Delta H_{\text{melt}} - \Delta H_{\text{cold cryst.}} \tag{2}$$

where ΔH^{o} is the heat of fusion of 100 crystalline polymer. The value for PEN is 103.4 J/g [8], and for PEEK is 130.0 J/g [19]. The apparent crystallinity of the crystallizable polymers in the blends can be normalized to the true crystallinity by dividing the apparent crystallinity with the fraction (in percent) of the crystallizable polymer.

The results are listed in Table 2.

2.7. Wide angle X-ray diffraction (WAXD)

To study the crystallization and orientation development in samples, wide angle X-ray diffraction technique was used.

2.7.1. WAXD profiles

A 12 kW Rigaku rotating anode generator (RU200B) equipped with a Rigaku horizontal diffractometer was used to obtain WAXD profiles of PEN/PEI/PEEK blends and oriented films. The X-rays were generated with copper target rotating anode with the generator being operated at 40 kV and 150 mA. The X-rays were monochromatized using a graphite monochromator to obtain the Cu K_α wavelength. The goniometer was operated with reflection mode by step scanning at a rate of 0.04°/step with a 5 s step interval.

2.7.2. WAXD film patterns

A General Electric copper target X-ray generator (GE XRD-6) equipped with a Furnas wide angle and small angle combination camera was used to obtain the wide angle X-ray diffraction patterns of PEN/PEI/PEEK blends, and oriented and annealed samples. The machine was operated at 30 kV and 30 mA and a nickel foil filter was used to obtain Cu K_α radiation. The distance between the sample and X-ray film plane is 32.19 mm. For biaxially oriented PEN/PEI/PEEK samples WAXD film patterns were obtained with X-ray beam in three directions: normal direction (ND), machine direction (MD), and transverse direction (TD).

2.8. Wide angle X-ray pole figure and biaxial orientation factors

Wide angle X-ray diffraction pole figures of selected, oriented and annealed PEN/PEI/PEEK films were obtained to evaluate the crystalline orientation of PEN in the blends with PEN-rich region (blends #6, #9, and #11). These were

Table 2
Thermal properties of PEN, PEI, PEEK

Materials	T_g (°C)	T_m (°C)	T_m^o (°C)	T_{cc} (°C)
PEN	123	258	337	223
PEI	218			
PEEK	146	340	384	173

T_m^o = equilibrium melting temperature.

performed using a GE XRD-6 X-ray generator equipped with a quarter circle goniometer and a goniometer head. The machine was operated at 30 kV and 30 mA to generate Cu K_α X-ray radiation. The sample was made to the dimension of $1.2 \times 1.2 \times 2.0$ mm cube by successively stacking the thin sample layers and binding them with super glue. The data were obtained by setting the experimental parameters of 10° interval for ϕ angle, 5° interval for azimuthal angle χ and typical counting time of 20–40 s at each point.

The White–Spruiell biaxial orientation factors [20] were used to evaluate the orientation of the crystalline regions. The value of the mean square cosine of the angle between the preferentially oriented axial and a reference axis was determined using Wilchinsky's method [21–23]. A pseudo-orthorhombic model [24] proposed for the PEN unit cell was used to calculate the orientation factor of the *c*-axis and the axis normal to the naphthalene plane. The calculations are as follows [12]:

c-axis:

$$\overline{\cos^2 \chi_{1c}} = 1 - 0.844\,\overline{\cos^2 \chi_1} - 1.156\,\overline{\cos^2 \chi_2} \tag{3}$$

axis normal to naphthalene plane

$$\overline{\cos^2 \chi_{1u}} = 1.022\,\overline{\cos^2 \chi_1} - 0.022\,\overline{\cos^2 \chi_2} \tag{4}$$

where $\overline{\cos^2 \chi_1}$ is obtained from (100) plane pole figure, $\overline{\cos^2 \chi_2}$ is obtained from (−110) plane pole figure.

3. Results and discussions

3.1. Thermal properties of PEN/PEI/PEEK blends

3.1.1. Differential scanning calorimetry (DSC)

3.1.1.1. Melt-cast PEN/PEI/PEEK sheets. Fig. 2 shows the effect of composition on the thermal behavior in melt-cast blends. From Fig. 2(a) for PEI-rich blends (samples #1, #2, and #3), we can see that neither cold crystallization nor melting peak of PEN appears during the DSC heating scan, suggesting that PEN stays in the amorphous state and remains completely miscible with PEI when the PEI concentration is more than 40 wt% and PEN concentration is less than 50 wt%. The glass transition temperature does not change significantly (~150 °C) with the change in composition. The melting temperature of PEEK increases with the increase of PEEK concentration. The cold crystallization temperature decreases with the increase of PEEK proportion, approaching that of 100% PEEK. This increase of T_{cc} with the addition of PEI is beneficial for film stretching as it widens the $(T_{cc} - T_g)$ gap where the optimum processing window lies. The area under the cold crystallization peak is roughly the same as that under the melting peak of PEEK indicating that the precursor samples are substantially amorphous.

Bicakci and Cakmak [16] performed the thermal analysis on extruded PEN/PEI/PEEK ternary blends. They found that in the compositions 1 (30/40/30), 2 (40/40/20) and 3 (50/40/10), only PEEK is able to crystallize, and PEN remains

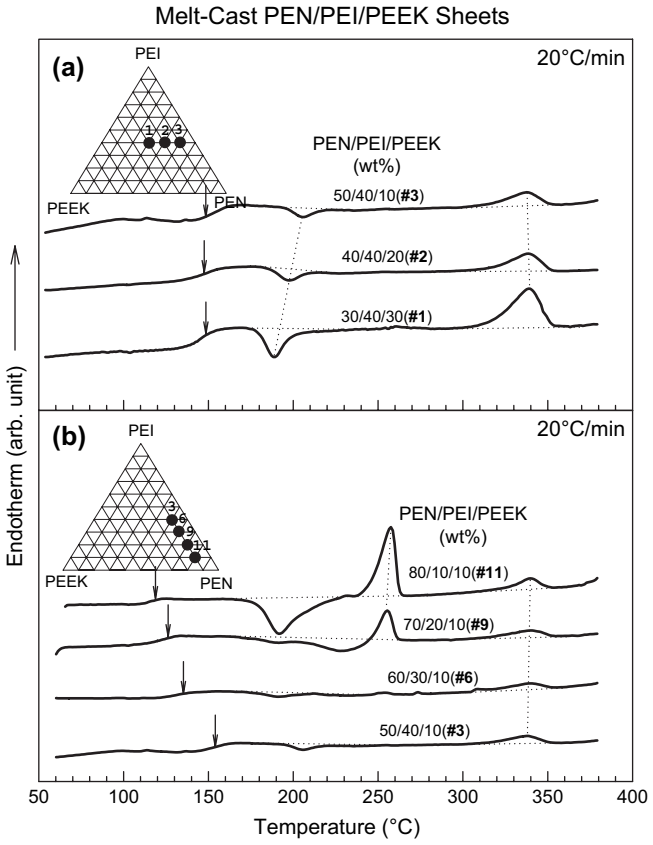

Fig. 2. DSC heating scans of melt-cast PEN/PEI/PEEK sheets.

amorphous throughout the DSC scan. This is very similar to that observed in the vitrified binary PEN/PEI blends where PEN is not able to crystallize in the blends containing more than 30% PEI during DSC heating scan with a heating rate of 10 °C/min [12]. This is primarily as a result of two processes: the dilution effect and the reduction of chain mobility. In the first process, the crystallizable chains are spatially separated by amorphous chains, and in the second process, the diffusion of the chains passed one another as characterized by self- and cross-diffusion coefficients decreased with the addition of amorphous chains.

Thermal behavior in PEN-rich region is shown in Fig. 2(b) for samples #3, #6, #9, and #11 with constant PEEK concentration of 10 wt%. The glass transition temperature increases with the increase of PEI fraction. The melting peak of PEN appears for samples #6, #9 and #11 which contain more than 60 wt% PEN, and the position of PEN melting peak decreases with the increase of PEI fraction. The melting peak of PEEK remains roughly the same (about 340 °C). In these DSC spectra, two overlapping cold crystallization peaks appear: the lower temperature peak corresponds to PEEK and the higher one to PEN. The reason why T_{cc} (PEEK) < T_{cc} (PEN) even though T_m (PEEK) > T_m (PEN), is because PEEK exhibits much higher crystallizability (thermally or stress induced). The area under the entire cold crystallization peaks is the same as that of the sum of the two individual melting peaks indicating that the precursors were amorphous prior to DSC scanning. One can also see that the cold crystallization peaks of PEN

and PEEK are overlapped, and the cold crystallization temperatures of both PEN and PEEK crystals increase with the increase of PEI fraction. Similar results have been found by the authors [18].

3.1.1.2. Effect of composition and annealing on the thermal properties of biaxially stretched films. Fig. 3 shows the DSC scans of samples #11, #9, #6, and #3 stretched at $T_g + 20$ °C with 3600%/min strain rate to a stretch ratio of 4×1, and subsequently annealed at 220 °C for 30 min. The cold crystallization temperature decreases as a result of increased chain orientation in the amorphous region. Oriented chains having lower entropy require less energy to crystallize. The blend films crystallize upon stretching due to stress induced crystallization. When the stretched films are annealed at 220 °C for 30 min (Fig. 3(b)), the cold crystallization peak disappears and the area under the melting peaks of both PEN and PEEK increases for all the films. This allowed us to calculate the crystallinity in these stretched and annealed samples. They are listed in Table 3. In the higher PEI concentration films (#3), PEN still remains amorphous upon stretching. Upon annealing it crystallizes, and a secondary melting peak close to the melting temperature of PEN appears. Kim et al. [12] and Buchner et al. [25] found the similar phenomena in crystallized and annealed PEN samples. This is attributed to the melting and recrystallization of poorly ordered and/or small crystallites into a higher order upon annealing.

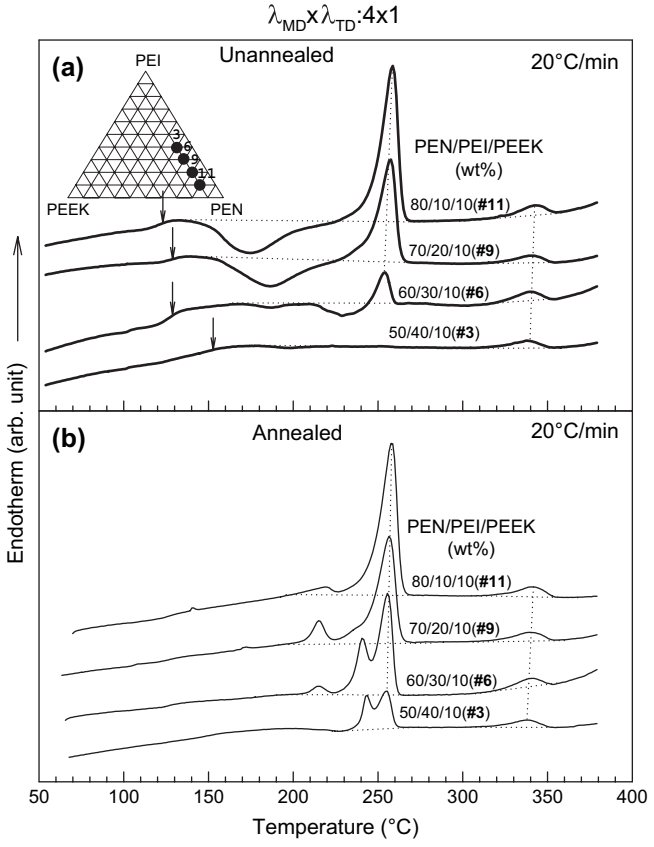

Fig. 3. DSC heating scans of PEN/PEI/PEEK films stretched at $T_g + 20$ °C with 3600%/min strain rate to stretch ratio of 4×1 (a) and subsequently annealed at 220 °C for 30 min (b).

Table 3
Thermal properties of PEN/PEI/PEEK blends

Sample (PEN/PEI/PEEK, wt%)	T_g (°C)	$T_{cc,PEEK}$ (°C)	$T_{cc,PEN}$ (°C)	$T_{m,PEN}$ (°C)	$T_{m,PEEK}$ (°C)
(a) Melt-cast sheets					
100/0/0	123.0	–	223.0	258.0	–
0/0/100	146.0	173.0	–	–	340.1
30/40/30 (#1)	145.5	188.9	–	–	338.8
40/40/20 (#2)	147.5	189.6	–	–	337.8
50/40/10 (#3)	151.1	–	201.6	–	337.3
60/30/10 (#6)	131.2	190.9	–	253.3	337.6
70/20/10 (#9)	120.2	190.9	226.8	255.5	339.6
80/10/10 (#11)	119.5	191.7	216.8	257.6	339.1
(b) PEN/PEI/PEEK films stretched at $T_g + 20$ °C with 3600%/min strain rate to stretch ratio ($\lambda_{MD} \times \lambda_{TD}$) of 4×1(unannealed)					
30/40/30 (#1)	149.4	–	–	–	340.53
40/40/20 (#2)	151.1	–	–	–	339.00
50/40/10 (#3)	151.9	–	–	–	337.7
60/30/10 (#6)	132.1	–	217.6	254.4	338.9
70/20/10 (#9)	125.1	187.9	212.0	257.1	339.0
80/10/10 (#11)	121.2	174.8	–	258.5	340.4

Sample (PEN/PEI/PEEK, wt%)	$T_{m,PEN}$ (°C)	$T_{m,PEEK}$ (°C)	Apparent crystallinity (%)	
			X_{PEN}	X_{PEEK}
(c) Stretched samples (in (b)) subsequently annealed at 220 °C for 30 min				
30/40/30 (#1)	241.2	341.1	0.71	9.42
40/40/20 (#2)	254.1	340.0	3.13	5.81
50/40/10 (#3)	255.1	337.5	5.81	2.06
60/30/10 (#6)	255.8	339.3	12.12	1.53
70/20/10 (#9)	256.6	338.9	17.43	2.31
80/10/10 (#11)	258.1	339.9	19.79	2.54

Fig. 4 shows the stretched (a) and annealed PEI-rich blend films (b) (blends #1, #2, and #3). The glass transition temperature does not change appreciably with stretching. PEN is in amorphous state in stretched films and it crystallizes upon annealing. The crystallinity of PEEK increases with the stretching primarily due to the stress induced crystallization as it will also be evident in X-ray data in the following sections. The corresponding data from thermal analysis on these samples are listed in Table 3.

3.1.1.3. Effect of uniaxial constant width (UCW) mode stretching and annealing on the thermal properties of PEN/PEI/PEEK films. Figs. 5 and 7 show the thermal behavior during DSC heating scan for 80/10/10 (#11) and 70/20/10 (#9) PEN/PEI/PEEK films stretched at $T_g + 20$ °C with 3600%/min strain rate to different stretch ratios (a) and subsequently annealed at 220 °C for 30 min (b). For sample #11 (80/10/10), the area under cold crystallization peaks becomes smaller (curves not shown) and T_{cc} (cold crystallization temperature peak position) decreases (Fig. 5) with the increase of area expansion ratio. This is a typical behavior observed in crystallizable polymers when stretched from amorphous precursors at temperatures between their glass transition and cold crystallization temperatures. With the increase of deformation, chain orientations increase, and during DSC scanning, these oriented

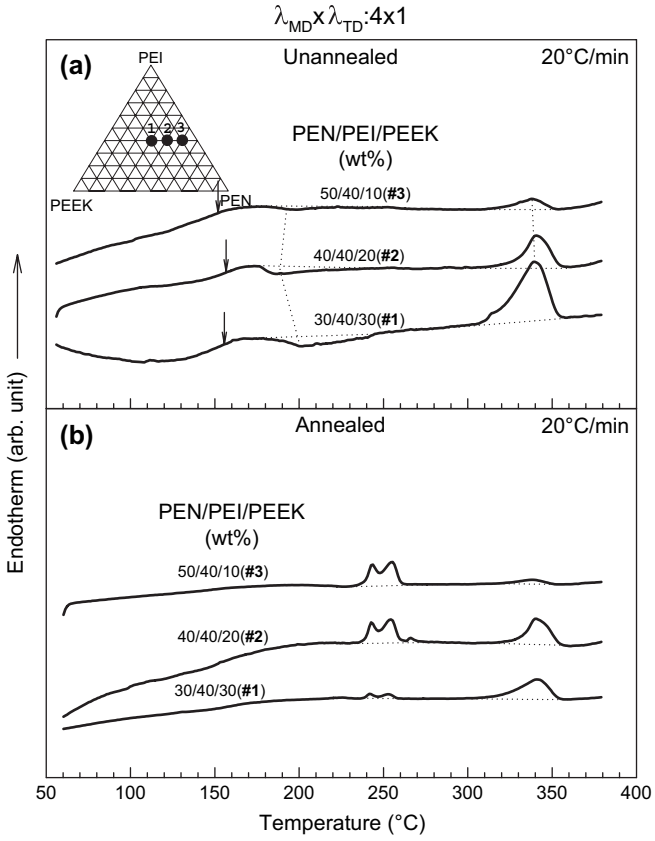

Fig. 4. DSC heating scans of PEN/PEI/PEEK films stretched at $T_g + 20$ °C with 3600%/min strain rate to stretch ratio of 4×1 (a) and subsequently annealed at 220 °C for 30 min (b).

amorphous regions require low thermal energy as a result of the reduction of conformational entropy and they crystallize at lower temperatures. This causes the shift of the cold

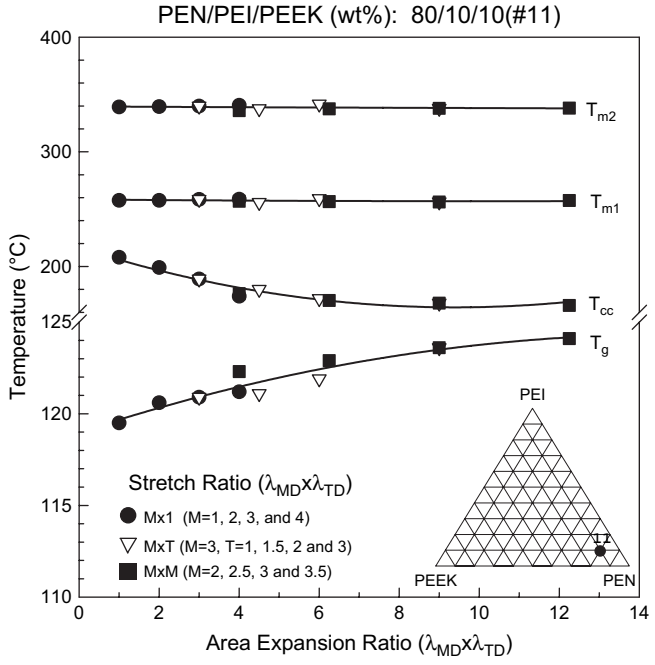

Fig. 5. Thermal properties as a function of area expansion ratio of PEN/PEI/PEEK films biaxially stretched at $T_g + 20$ °C with 3600%/min strain rate.

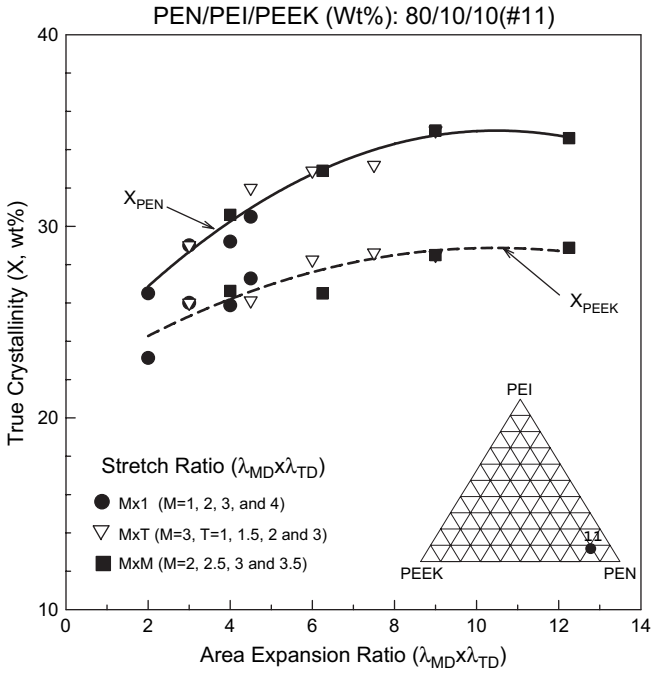

Fig. 6. True crystallinity as a function of area expansion ratio of PEN/PEI/PEEK films biaxially stretched at $T_g + 20$ °C with 3600%/min strain rate.

crystallization temperature to lower temperatures as the fraction of the remaining amorphous chains decreases upon crystallization due to heating. Crystallinity of the stretched films could not be calculated. Although there are two melting peaks, only one cold crystallization peak is present. Therefore, the signals coming from PEEK and PEN crystallization could not be separated. When these stretched films are annealed, however, the cold crystallization peaks disappear, and this allowed us to calculate the crystallinity for annealed films as shown in Fig. 6 where the true crystallinity (normalized to their fraction present) in each phase is plotted with area expansion ratio. These data do not depend on the mode of deformation and the PEEK phase exhibits lower crystallinity than in PEN phase as it is understandable as the PEEK chains are widely dispersed in PEI/PEN.

When the concentration of PEI is increased at a constant PEEK fraction (10 wt%) in sample #9 (70/20/20) as shown in Figs. 7 and 8, the same trends as seen in sample #11 are observed. The same results have been found in the uniaxially stretched PEN/PEI/PEEK blends [18]. Increase of area expansion ratio results in the decrease of the cold crystallization temperature and an increase in its breadth (not shown), while substantial increase in glass transition temperature is observed. The latter result points to the substantial stiffening of the chains in the amorphous domains in large part due to the development of orientation. In these samples, as soon as the chains attain sufficient mobility, they rapidly crystallize with those chains in the amorphous state having highest orientation and are spatially in close proximity (Fig. 8).

With the increase of PEI concentration to 40 wt% in sample #2 (40/40/20), the crystallizability, particularly in the PEN phase is reduced, as shown in Fig. 9(a). We could not observe

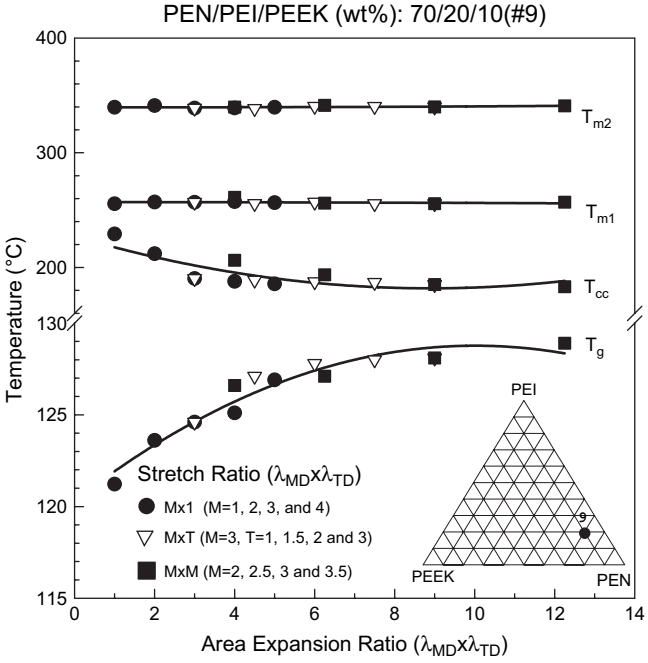

Fig. 7. Thermal properties as a function of area expansion ratio of PEN/PEI/PEEK films biaxially stretched at $T_g + 20$ °C with 3600%/min strain rate.

cold crystallization and melting peaks of PEN, but the PEEK phase shows crystallization and melting peaks. The area under the cold crystallization peaks decreases with stretching while the area under the melting peak increases indicating increased crystallinity in the PEEK phase upon stretching. We also see that a large portion of the crystallizable material remains amorphous even at high stretch ratios. As we will see in the X-ray section, these films exhibit only oriented PEEK phase. No

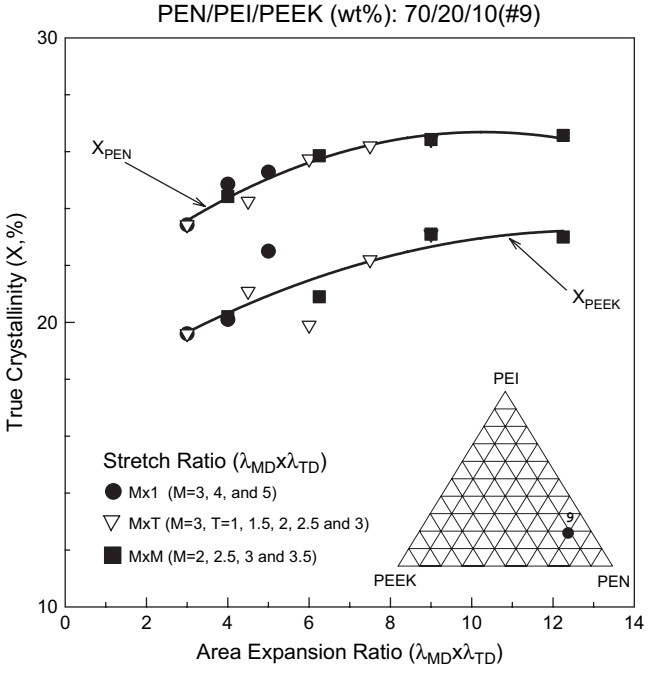

Fig. 8. True crystallinity as a function of area expansion ratio of PEN/PEI/PEEK films biaxially stretched at $T_g + 20$ °C with 3600%/min strain rate.

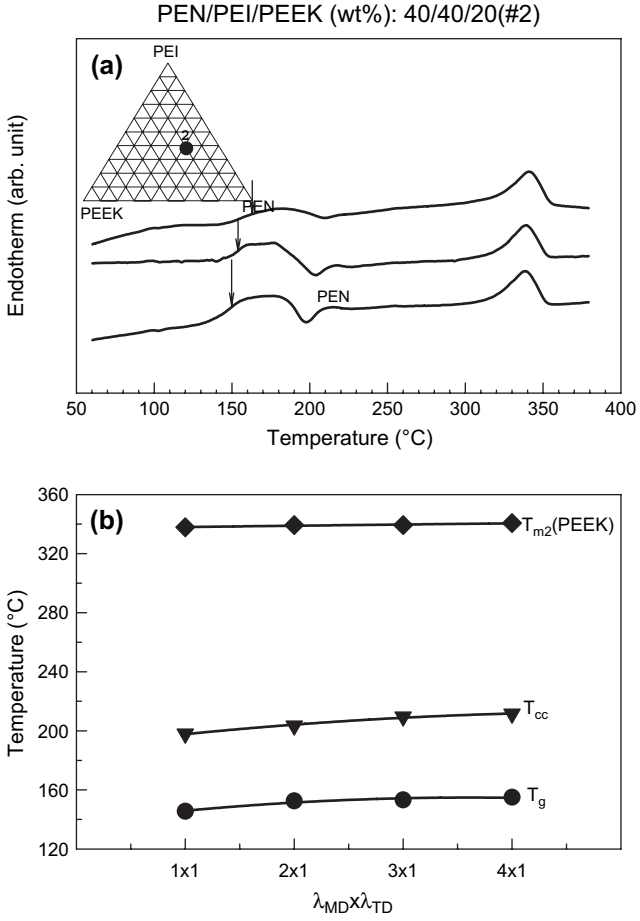

Fig. 9. DSC heating scans (a) and thermal properties (b) of PEN/PEI/PEEK films stretched at $T_g + 20$ °C with 3600%/min strain rate to different stretch ratios.

evidence of PEN crystallites is observed indicating that PEN chains remain well mixed with PEI. The glass transition temperature, cold crystallization temperature, and the melting temperature are plotted as a function of stretch ratio in Fig. 9(b). The melting temperatures of PEEK do not change appreciably with the increase of stretch ratios. The glass transition temperature and the cold crystallization temperature increase upon stretching.

3.2. Wide angle X-ray diffraction (WAXD)

In order to determine the structural evolution during stretching, two wide angle X-ray diffraction techniques have been employed: WAXD equatorial scan and WAXD flat film patterns. WAXD film patterns were obtained with X-ray beam normal to the film surface in the case of uniaxially free-width stretched sample while in the case of biaxially stretched films three WAXS patterns were obtained with the X-ray beam in three principal directions MD, TD and ND.

3.2.1. WAXD equatorial intensity profiles

As-cast films are all amorphous as discussed in Section 2.6. Upon stretching, the crystalline peaks of PEN and PEEK start to appear as shown in Fig. 10(a) in the blends of samples #11

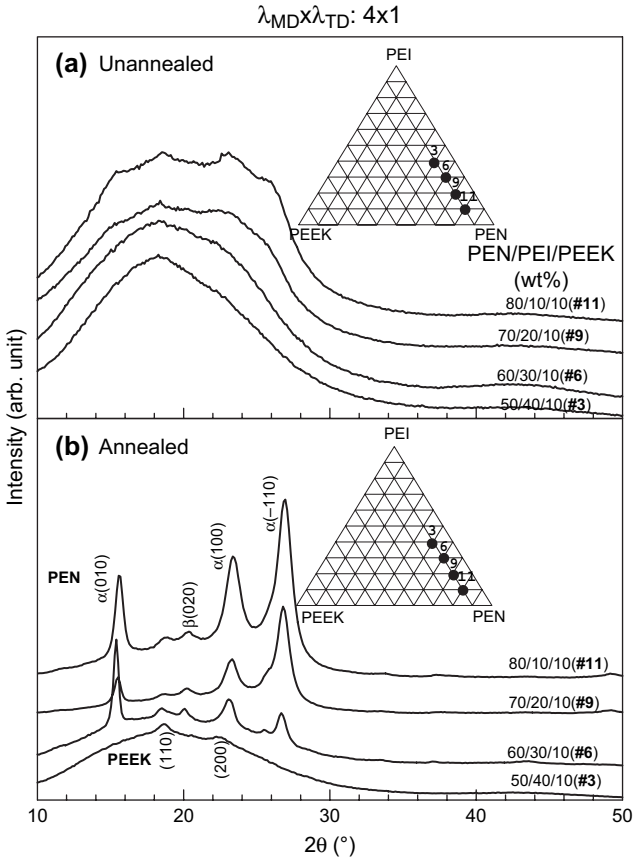

Fig. 10. WAXD equatorial intensity profiles from PEN/PEI/PEEK films stretched at $T_g + 20\,^{\circ}C$ with 3600%/min strain rate to stretch ratio of 4×1. (a) Unannealed and (b) annealed at 220 °C for 30 min.

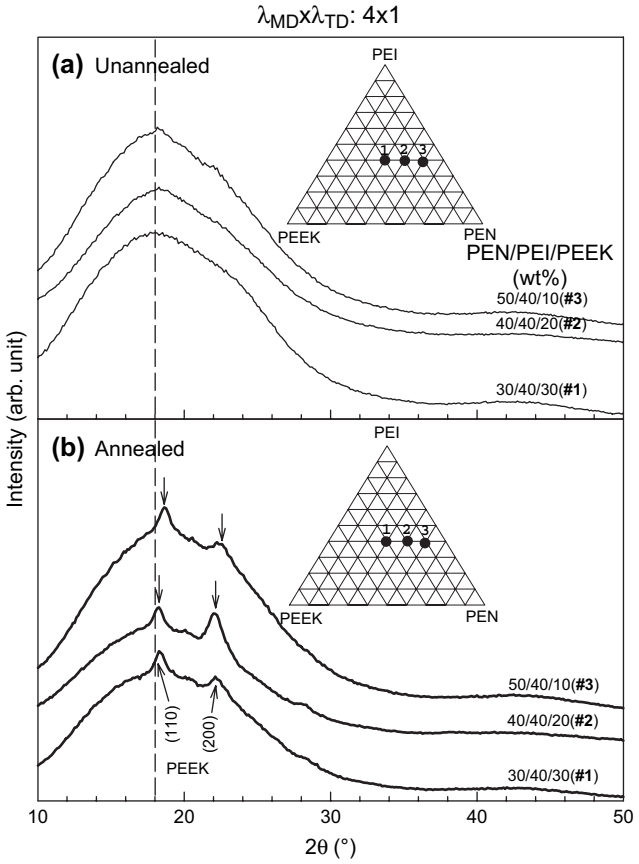

Fig. 11. WAXD equatorial intensity profiles from PEN/PEI/PEEK films stretched at $T_g + 20\,^{\circ}C$ with 3600%/min strain rate to stretch ratio of 4×1. (a) Unannealed and (b) annealed at 220 °C for 30 min.

and #9, which contain a higher proportion of crystallizable components. The samples with higher PEI content (samples #6 and #3), remain amorphous even at 4×1 deformation level. When these stretched samples are annealed, the crystalline peaks appear in samples #1, #2, and #3 (Fig. 11 (b)), and they become very strong in samples #6, #9 and #11. The low temperature modification α of PEN is predominant in samples #11 and #9 (Fig. 10 (b)). In samples #1, #2, and #3, only PEEK crystalline peaks are observed. Only in sample #6 composition both PEEK and PEN crystalline peaks are observed.

As indicated earlier in Section 2.6, the as-cast precursor sheets are all amorphous for the composition range studied. Stress induced crystallization of PEN occurs in PEN-rich films. Although its relative proportion is low (10−30%), PEEK stress crystallizes in samples #1−3 composition. Annealing increases the crystallinity of PEN and PEEK in deformed films. In order to probe the structure evolution and crystalline orientation during the stretching and annealing, WAXD film patterns were obtained as presented in the following section.

3.2.2. WAXD film patterns

Fig. 12 shows the WAXD patterns of uniaxial constant width stretched (stretch ratio $= 4 \times 1$) #11 and #2 films. These patterns were obtained with the X-ray incident direction in its normal direction after the stretched samples were annealed. PEN crystal planes were identified by comparing *d*-spacing values with the literature [18]. PEEK crystal (orthorhombic) planes were identified by comparing experimental *d*-spacing values with the ones calculated based on the lattice parameters of Dawson and Blundell [26] listed in Table 4.

As we can see from these patterns, in PEN-rich #11 film, the low temperature modification α of PEN is the only phase. Among all diffracted peaks, (010), (100) and (−110) peaks show very strong intensity. There exists a weak diffraction in between α(010) and α(100) on the equator. Bicakci and Cakmak [16] indicated that in uniaxial free-width stretched samples, a weak diffraction in between α(010) and α(100) on the equator is due to (110) plane diffraction of PEEK. We compared our observed *d*-spacing value of PEN ($d_{\beta(020)} = 4.79$) with the value from the literature [2,3,7] ($d_{\beta(020)} = 4.78$) which are very close to each other, while the calculated *d*-spacing of the PEEK (110) plane is 4.679. Therefore, we concluded that this weak peak is due to β(020) of PEN. One possible interpretation for this weak β peak is that the stretched sample was annealed at 220 °C which is close to the melting temperature of PEN, at which the PEN prefers to form a mixture of α and β [12,27]. In sample #2 diffraction pattern, only PEEK peaks appear, and (110), (200) peaks on the equator and (111) peak on first layer line are visible. There are no crystalline peaks of PEN shown in this sample. This is in agreement

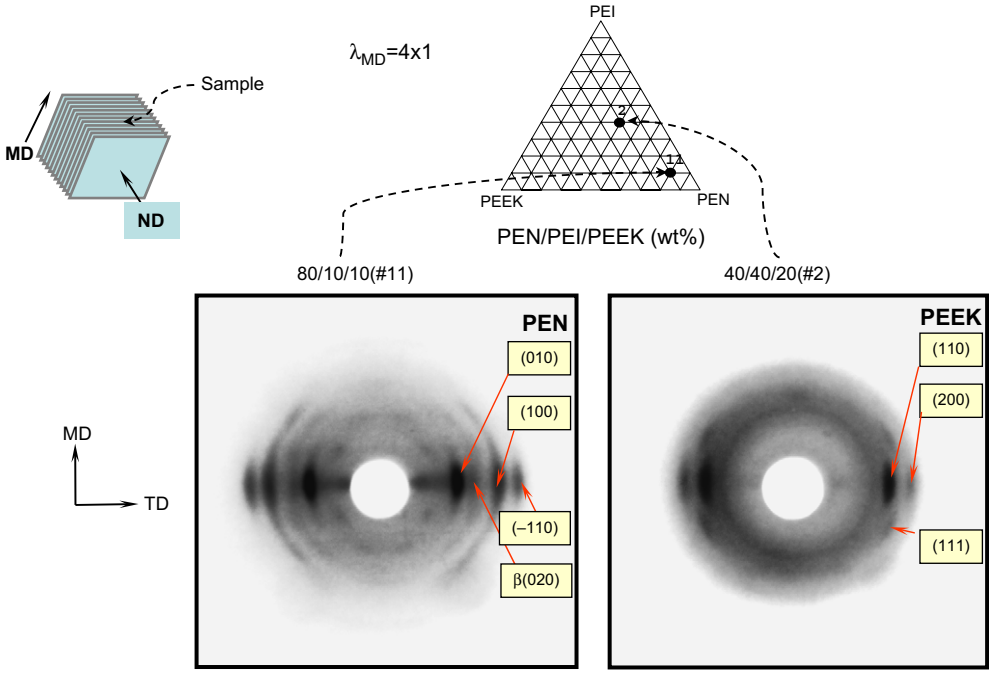

Fig. 12. WAXD patterns of 80/10/10 (#11) and 40/40/20 (#2) PEN/PEI/PEEK films stretched at $T_g + 20$ °C with 3600%/min strain rate to stretch ratio of 4 × 1 and subsequently annealed at 220 °C for 20 min.

Table 4
Calculated *d*-spacing values of PEEK

Planes	*d* (calculated)
(110)	4.679
(200)	3.875
(111)	4.230

with the results of uniaxial free-width samples observed by Bicakci et al. [18,19].

In order to systematically investigate the effect of composition, stretch ratio, stretching mode and annealing on the crystallization and crystalline orientation, a series of WAXD patterns were obtained. Figs. 13 and 14 show the effect of composition and annealing on the crystallization and orientation of uniaxial

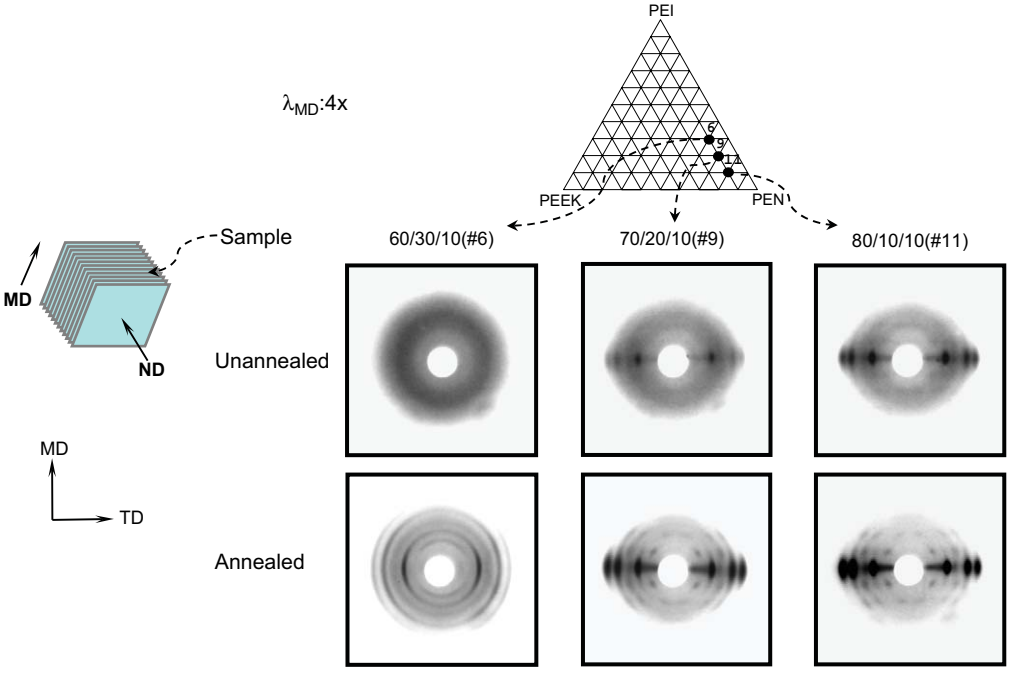

Fig. 13. WAXD patterns of PEN/PEI/PEEK blends uniaxially stretched at $T_g + 20$ °C with 3600%/min strain rate to stretch ratio of 4× and subsequently annealed at 220 °C for 20 min.

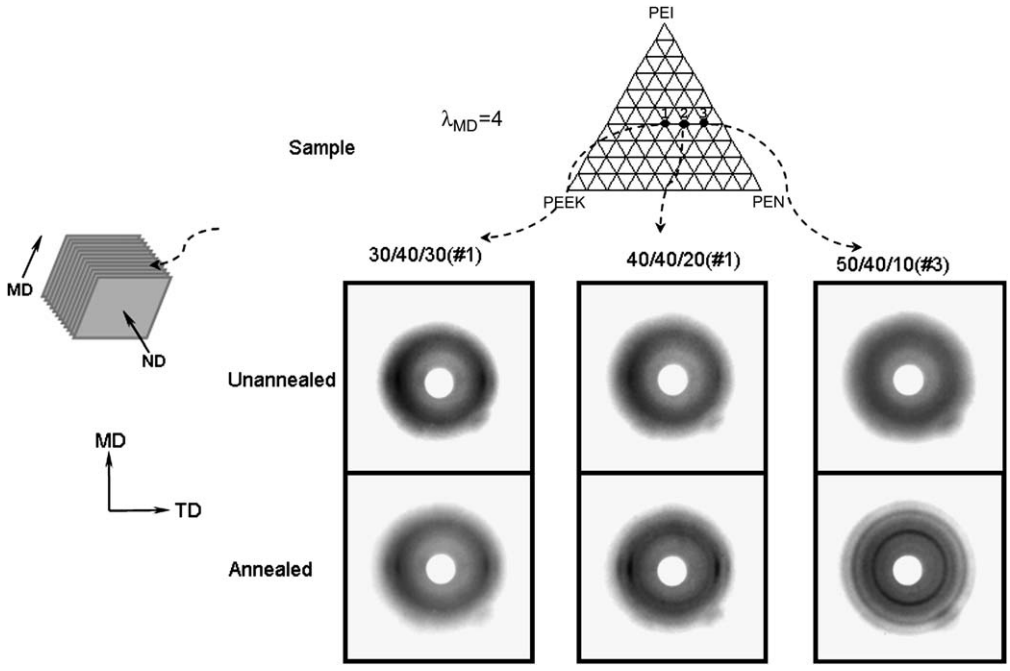

Fig. 14. WAXD patterns of PEN/PEI/PEEK blends stretched at $T_g + 20$ °C with 3600%/min strain rate to stretch ratio of 4× and subsequently annealed at 220 °C for 20 min.

free-width stretched films for PEN-rich (samples #6, #9, and #11) and PEI-rich films (samples #1, #2, and #3), respectively. The stretch ratio of these films is 4. In sample #11, the sharp equatorial spots with small azimuthal spread are observed. Crystallization and crystal orientation are high in this sample. Annealing enhances the crystallization in the film. Similar behavior is observed in sample #9 even though the PEI proportion is increased to 20 wt%. The azimuthal spread in these crystalline peaks increases with the addition of the PEI proportion. With further addition of PEI to 30 wt% at the expense of PEN in the sample #6, the formation of crystalline lattice is severely retarded. The molecular chains are randomly oriented in the amorphous matrix for unannealed film suggesting that the chain orientation of PEN is disrupted by the bulky chains of PEI. This behavior is quite understandable. As the fraction of non-crystallizable PEI phase is increased, the dilution effect spatially separates the crystallizable chains from one another [18].

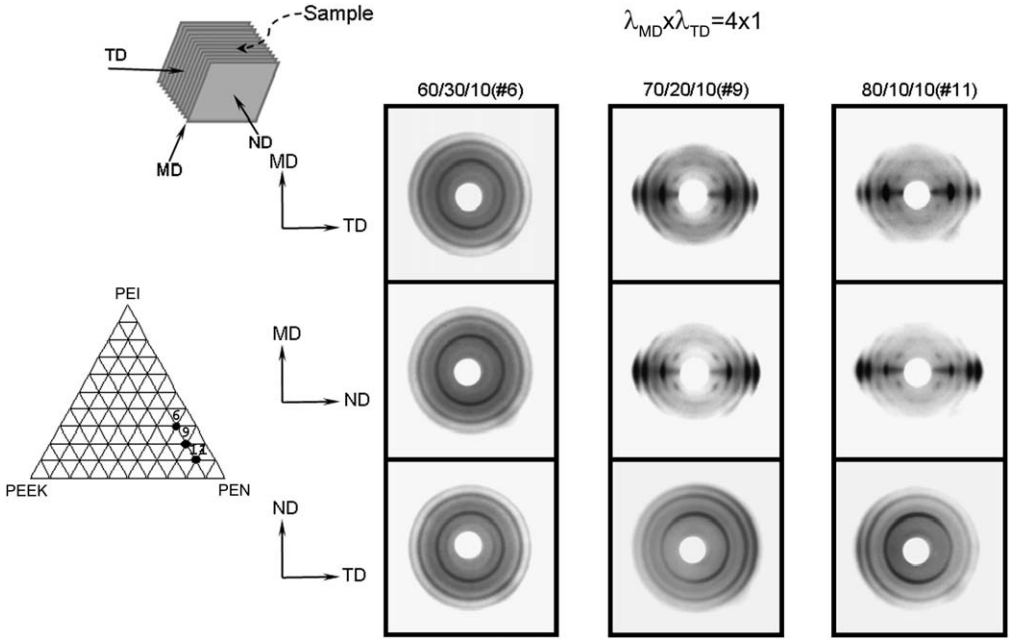

Fig. 15. WAXD patterns of PEN/PEI/PEEK blends stretched at $T_g + 20$ °C with 3600%/min strain rate to stretch ratio of 4 × 1 and subsequently annealed at 220 °C for 20 min.

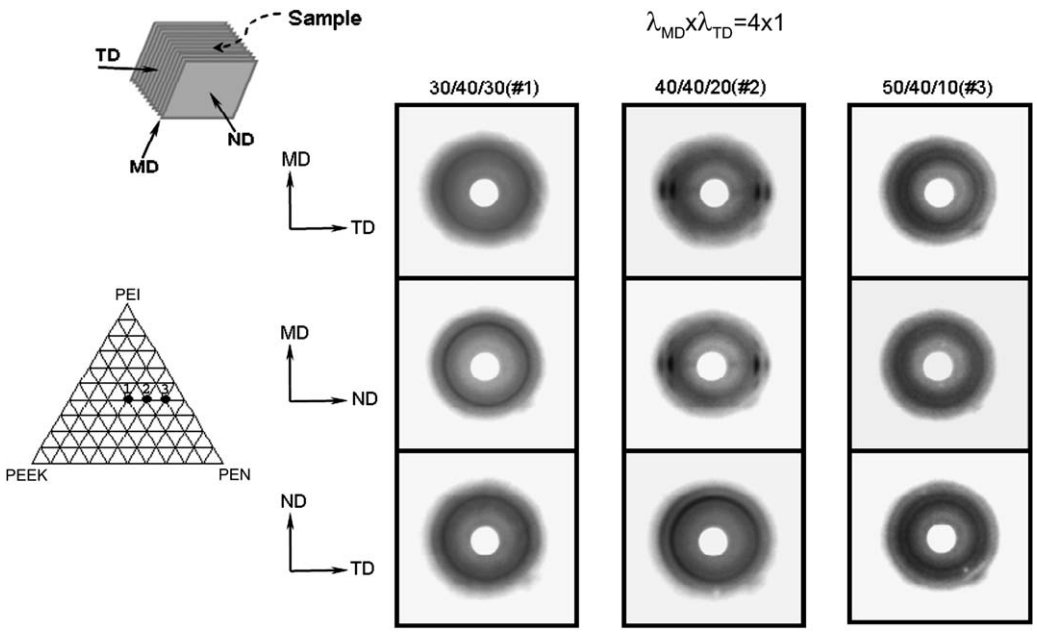

Fig. 16. WAXD patterns of PEN/PEI/PEEK blends stretched at $T_g + 20$ °C with 3600%/min strain rate to stretch ratio of 4 × 1 and subsequently annealed at 220 °C for 20 min.

In Figs. 15 and 16, we show the effect of the composition on crystalline orientation for PEN-rich samples (samples #11, #9, and #6) and PEI-rich samples (samples #1, #2, and #3) uniaxial constant width (UCW) stretched to the stretch ratio of 4 × 1. These WAXD patterns were obtained with an X-ray beam in ND, MD, and TD directions. Crystallization and crystalline orientation increase with the addition of PEN. Transverse isotropy is observed with highly oriented α phase crystals of PEN in samples #11 and #9. For sample #6, unoriented crystals in the blend are formed during annealing. These crystals correspond to both PEN and PEEK. This orientation behavior is quite similar to that of the uniaxial free-width stretched sample as discussed in the previous section. As in the case of the unannealed samples, samples #11 and #9 have predominately PEN crystals while sample #6 has a combination of PEN and PEEK crystals. During the annealing process where they obtain the necessary energy, PEN chains which were oriented but not packed into a crystal lattice in as-stretched films rearrange

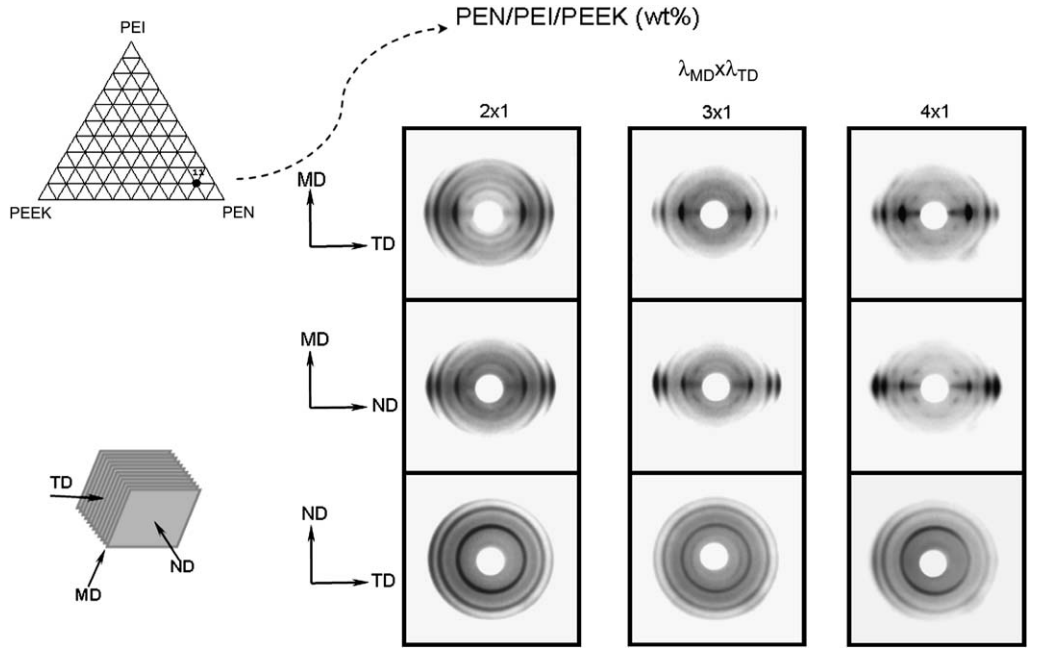

Fig. 17. WAXD patterns of 80/10/10 (#11) PEN/PEI/PEEK blends stretched at $T_g + 20$ °C with 3600%/min strain rate to different stretch ratios and subsequently annealed at 220 °C for 20 min.

and subsequently crystallize. With the further increase of PEI fraction to 40 wt% in samples #1, #2, and #3 (Fig. 16), all the crystalline peaks observed in WAXD patterns belong to PEEK even though these blends contain substantial fraction of PEN and PEI, particularly in samples #1 and #2. Similar results have been reported by Bicakci and Cakmak [16] for uniaxially stretched and annealed films. In PEI-rich blends (samples #1, #2, and #3), the overall crystallinity and the crystal orientation are low except for the sample #2 which is 40/40/20 wt% of PEN/PEI/PEEK.

Figs. 17 and 18 show the effect of the stretch mode and stretch ratio on the structure evolution in sample #11 under

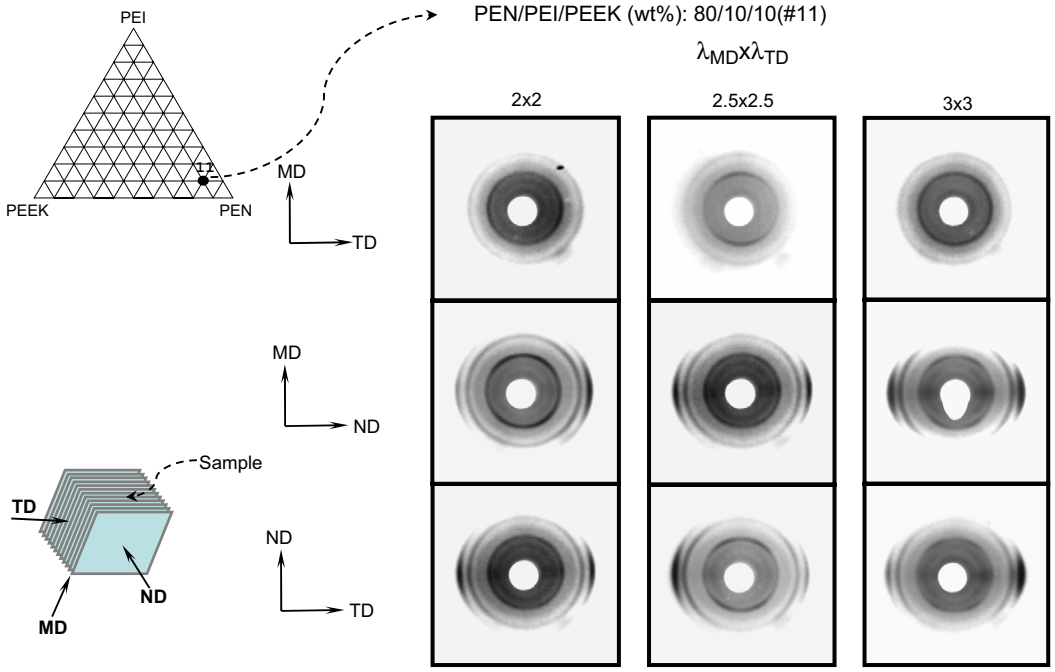

Fig. 18. WAXD patterns of 80/10/10 (#11) PEN/PEI/PEEK blends stretched at $T_g + 20$ °C with 3600%/min strain rate to different stretch ratios and subsequently annealed at 220 °C for 20 min.

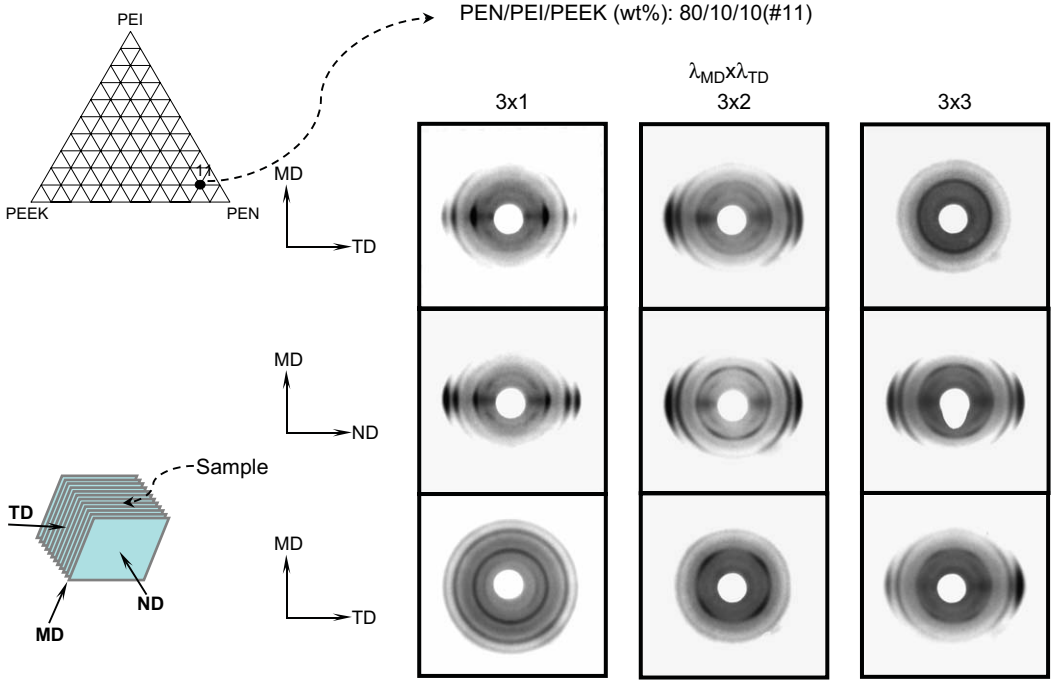

Fig. 19. WAXD patterns of 80/10/10 (#11) PEN/PEI/PEEK blends stretched at $T_g + 20$ °C with 3600%/min strain rate to different stretch ratios and subsequently annealed at 220 °C for 20 min.

different stretching modes. Crystallinity and crystal orientation increase with the stretch ratio in the samples stretched under all three different stretching modes. As indicated in our earlier publication [27], when the films are stretched in UCW (uniaxial constant width) mode, with very high stretch rate (3600%/min), they exhibit a texture very close to transverse isotropy, as indicated by the similarity of WAXD patterns obtained with the X-ray beam along the ND and TD as we can see from Fig. 17. In the case of unequal biaxial (UB) stretching shown in Fig. 19, PEN exhibits bimodal orientation as indicated by the presence of two (010) populations: one is observed in the transverse direction, the other in the machine direction. In equal biaxial condition shown in Fig. 18, this bimodal behavior disappears and in-plane isotropy is observed. This behavior can be further confirmed by wide angle X-ray pole figure analysis as discussed in the following section.

3.3. Wide angle X-ray pole figure analysis

3.3.1. Effect of the composition on biaxial orientation

Figs. 20 and 21 show the WAXD pole figure contour plots and three dimensional plots for #11, #9 and #6 films uniaxially stretched at $T_g + 20$ °C with 3600%/min strain rate to stretch ratios of 3×1 and 3×3 and subsequently annealed at 220 °C for 30 min. It is indicated that the *c*-axis of PEN chain (as represented by (010) plane) oriented in TD−ND plane which concentrated slightly in TD in the case of 3×1. When the films are equally biaxially stretched (3×3 in Fig. 21), the *c*-axis of PEN shows bimodal orientation. Naphthalene planes which are represented by (−110) plane of PEN progressively concentrated in the normal direction, in the case of 3×1 and especially 3×3. When PEI fraction is increased in the blends, the orientation for both *c*-axis and naphthalene planes decreases.

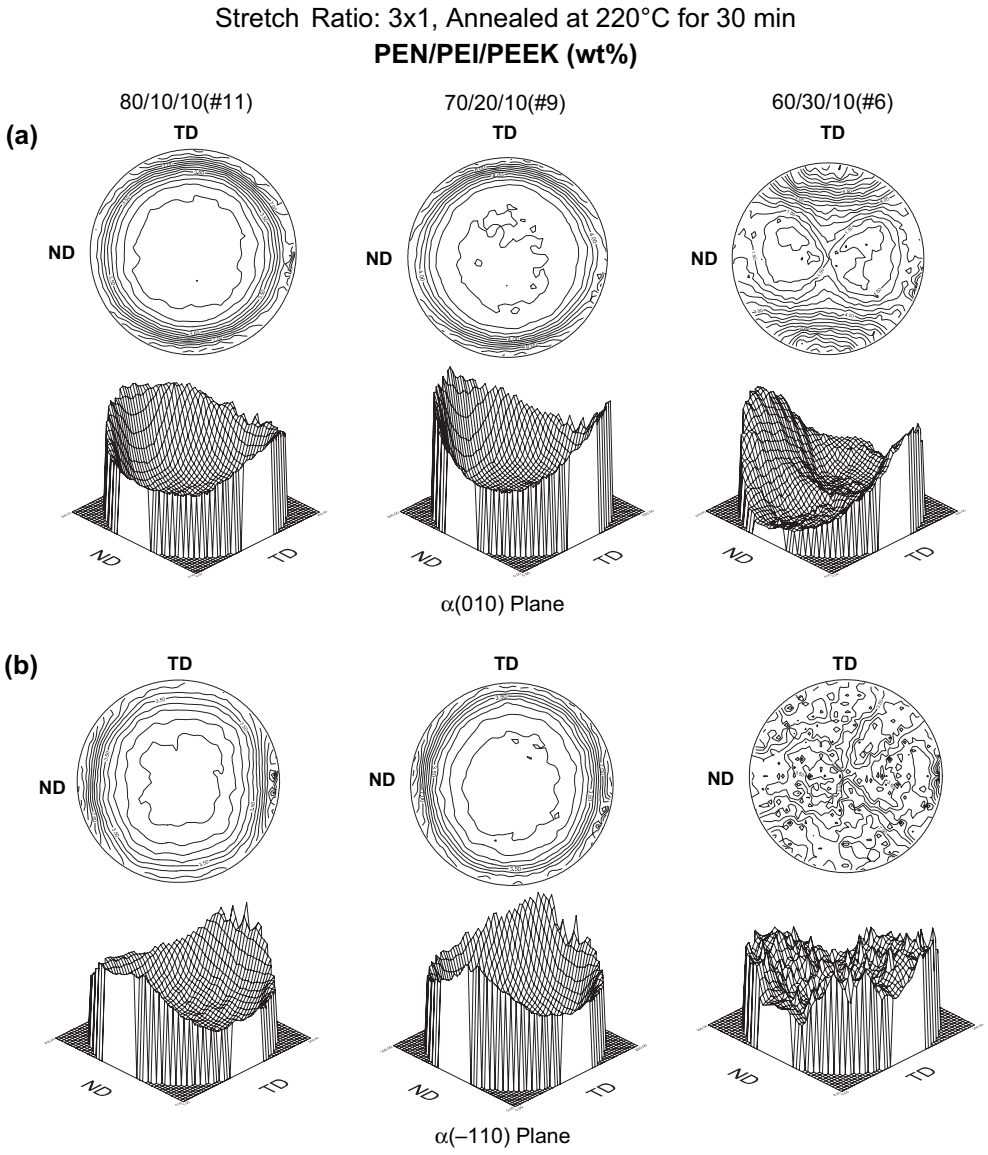

Fig. 20. 3D WAXS pole figures and isointensity contour plots of PEN (a) (010) plane and (b) (−110) plane of films stretched at $T_g + 20$ °C with 3600%/min strain rate to 3×1 stretch ratio and subsequently annealed at 220 °C for 30 min.

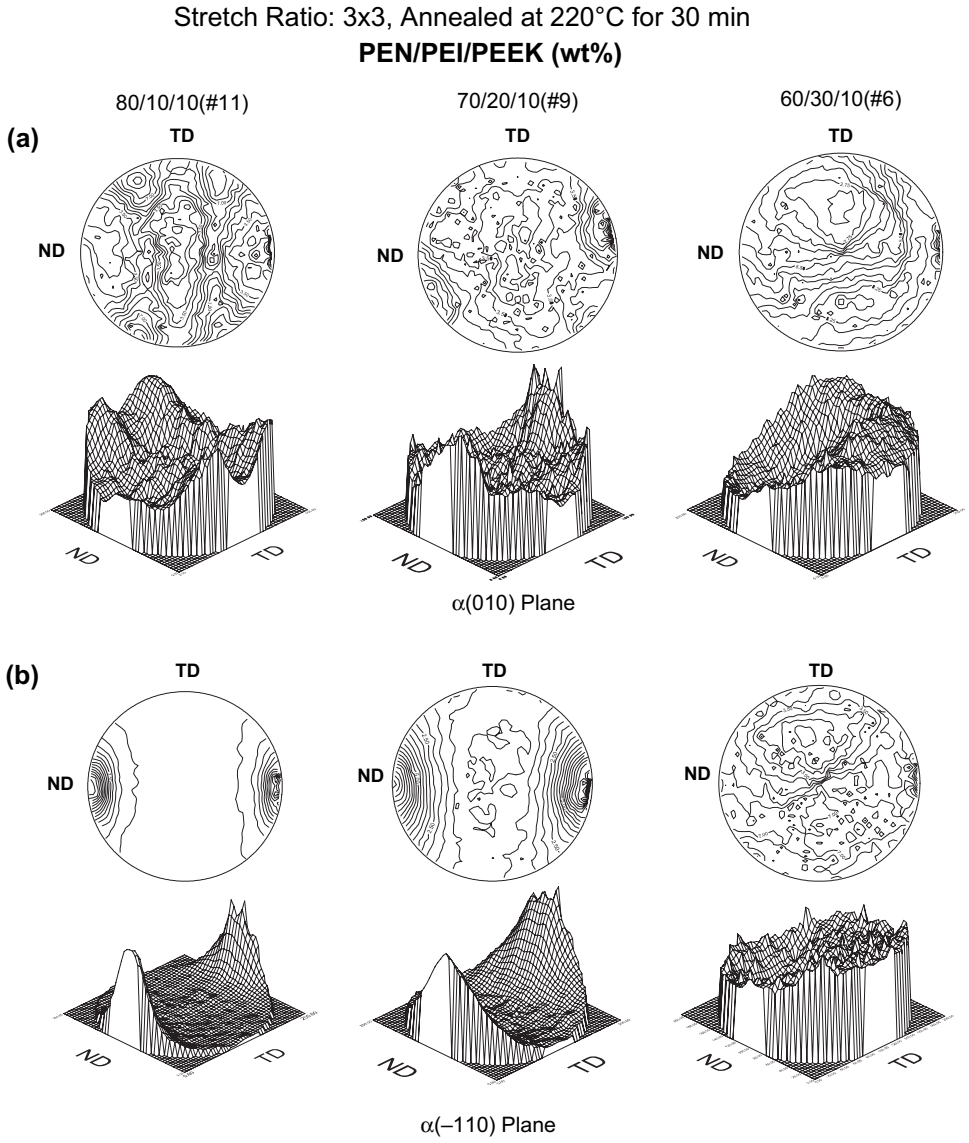

Fig. 21. 3D WAXS pole figures and isointensity contour plots of PEN (a) (010) plane and (b) (−110) plane of films stretched at $T_g + 20$ °C with 3600%/min strain rate to 3×3 stretch ratio and subsequently annealed at 220 °C for 30 min.

In order to obtain detailed information about the effect of PEI on the crystalline orientation, White−Spruiell biaxial orientation factors were calculated from the pole figure data. Fig. 22 shows the White−Spruiell biaxial orientation factors of the *c*-axis and the axis normal to the naphthalene plane for 3×1 and 3×3 stretch ratios of samples #11, #9 and #6. For 3×1 films the orientation factors lie close to the vertical axis indicating that 3×1 films are generally uniaxial in character. For 3×3 films, the orientation factors lie on the diagonal line which is an equi-biaxial orientation condition indicating that all the films experienced balancing stretching in MD−TD plane. With the increase of PEI, the orientation factor of the *c*-axis and the axis normal to the naphthalene plane moves towards the isotropic point which is the origin of the coordinate along the diagonal line. This suggested that the presence of bulky PEI molecules disturbs the preferential orientation of *c*-axis towards the machine direction and the naphthalene plane parallel to the film surface. Similar trends were observed [12] in the case of PEN/PEI blends. This hindrance to preferential orientation of naphthalene groups by the amorphous PEI chains results in conversion of bimodal orientation behavior to in-plane isotropy in biaxially stretched films.

3.3.2. Effect of stretch ratio and stretching mode on biaxial orientation

Fig. 23 shows the contour plots and 3D pole figures for sample #11 uniaxial constant width stretched and annealed films. Uniaxial free-width stretched sample 4× exhibits transverse isotropy as evidenced by the uniform distribution of intensity in ND−TD plane. This transverse isotropy is no longer present while the width is kept constant. In this figure, the increase in λ_{MD} concentrate (−110) poles in ND and (010) poles in TD. The orientation of (−110) planes which are almost parallel to the naphthalene planes ($\sim 7^\circ$) was observed previously [12].

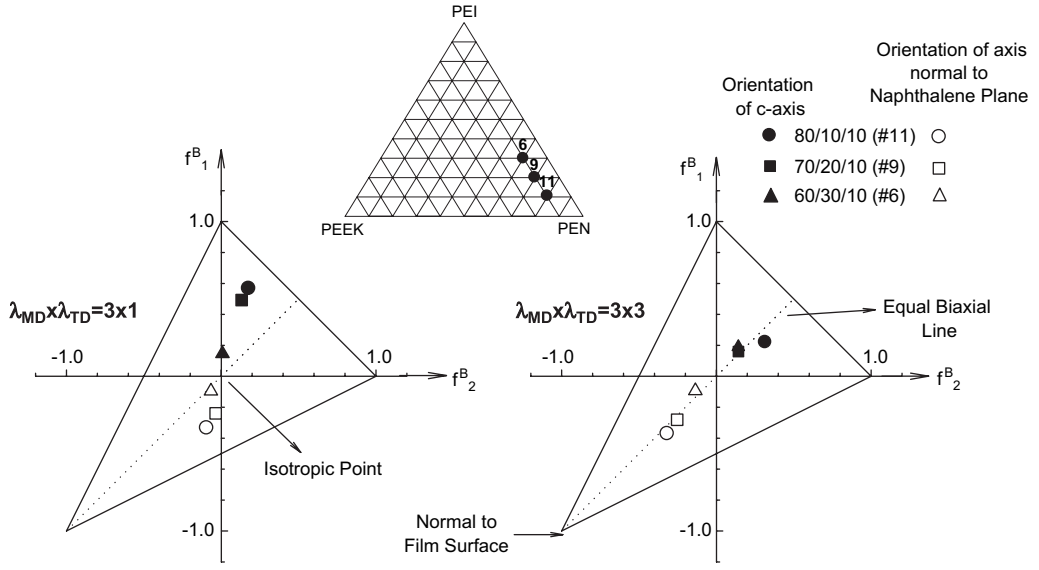

Fig. 22. White–Spruiell orientation function for *c*-axis and the axis normal to the naphthalene planes of deformed PEN/PEI/PEEK films after annealing.

In unequal biaxially stretched sample (3×2) as shown in Fig. 24, the poles of (010) plane begin to show bimodal orientation (see four distinct peaks). The bimodal orientation for the *c*-axis increases significantly when the equal biaxial stretch ratio increases (3×3 and 3.5×3.5), and the naphthalene plane orients parallel to the film surface progressively. The orientation factors for the *c*-axis and the axis normal to the naphthalene plane are plotted in Fig. 25. The magnitude of the orientation factors increases with the λ_{MD}, and they move towards the equi-biaxial line as the films are stretched under UB mode and eventually closer to the diagonal line when the balancing stretch condition is attained.

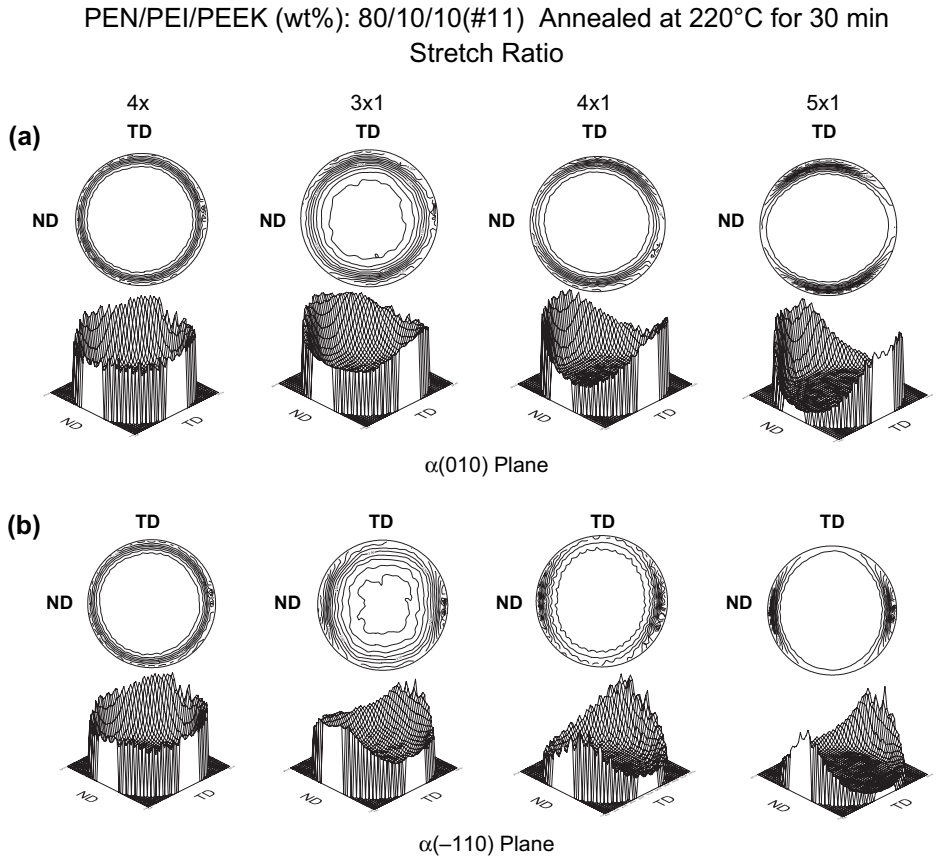

Fig. 23. 3D pole figures and contour plots of (a) PEN (010) plane and (b) PEN (−110) plane of 80/10/10 (#11) films stretched at $T_g + 20$ °C with 3600%/min strain rate and subsequently annealed at 220 °C for 30 min.

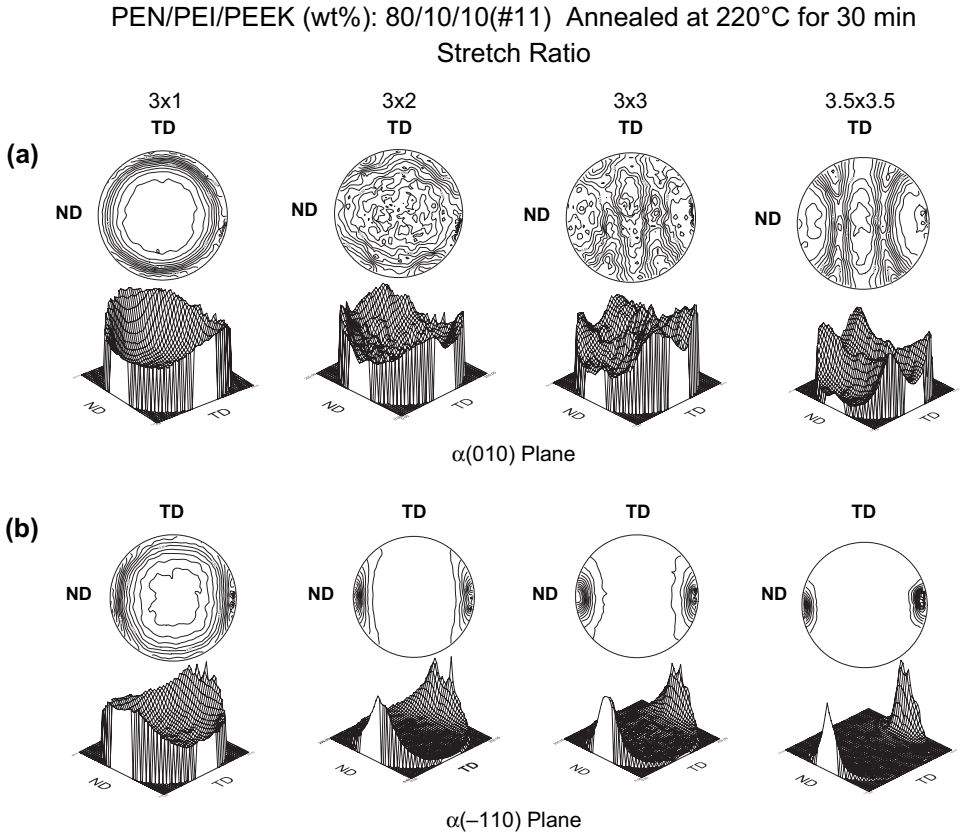

Fig. 24. 3D pole figures and contour plots of (a) PEN (010) plane and (b) PEN (−110) plane of 80/10/10 (#11) films stretched at $T_g + 20$ °C with 3600%/min strain rate and subsequently annealed at 220 °C for 30 min.

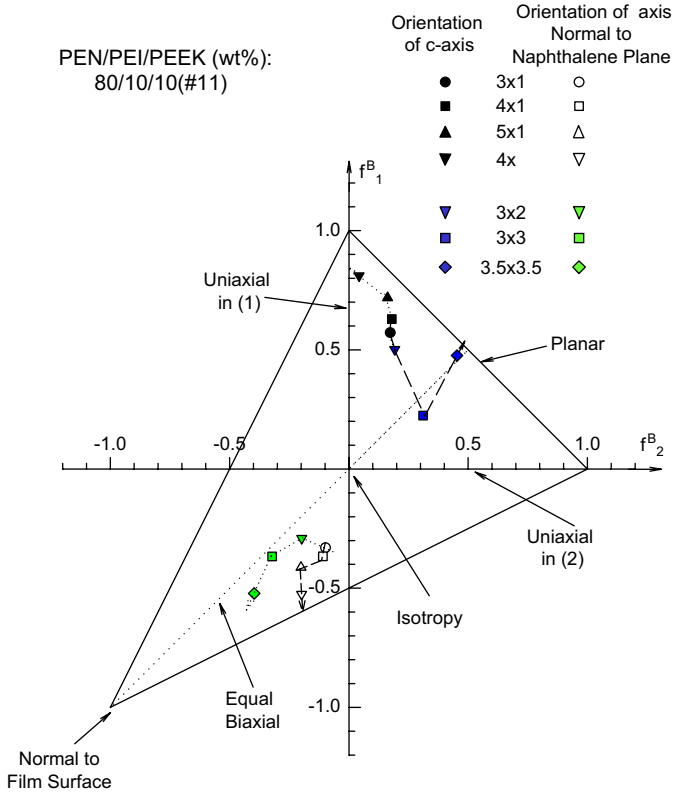

Fig. 25. White–Spruiell orientation function for *c*-axis and the axis normal to the naphthalene plane.

4. Conclusions

The effect of biaxial stretching and annealing on the structure development in ternary blends of PEN/PEI/PEEK on mostly PEN-rich compositions has been investigated. The results confirm that PEN/PEI and PEEK/PEI binary pairs are melt miscible. This results in single T_g when rapidly quenched. The addition of PEI to PEN greatly suppresses the crystallizability that disappears at about 20% altogether. The addition of PEEK to high PEI containing PEN/PEI recovers this strain crystallizability leading to a strain hardenable films in the rubbery stretching temperatures. The crystalline texture in the PEN-rich films resulting from annealing exhibits cross-hatched morphology, the increase of PEI concentration eliminates this cross-hatched morphology presumably by increasing the interchain friction between the PEN chains. The crystallization habit is mostly PEN at PEN-rich corner of the ternary diagram. The increase of PEI concentration beyond 20% eliminates the crystallizability of PEN and addition of as little as 10% PEEK causes these blends to crystallize upon stretching. All of the PEN/PEI/PEEK films that biaxially stretched in rubbery state were found to be necking free.

References

[1] Sebahar J. Modn Plast Encycl'97, B-61; 1997.
[2] Anon. Res Disc 1987;283:735.

[3] Ono K. Jap Pat No 87/198445; 1987.
[4] Sakamoto S, Sato Y. Eur Patent App No 229255 A2; 1987.
[5] Utsumi S. Jap Patent No 87/135339; 1987.
[6] Kojima K, Takai Y, Ieda M. J Appl Phys 1986;59(8):2655.
[7] Mencik Z. Chem Prum 1976;17.
[8] Buchner S, Wiswe D, Zachmann HG. Polymer 1989;30:480.
[9] Cakmak M, Wang YD, Simhambhatla M. Polym Eng Sci 1990;30:721.
[10] Murakami S, Nishikawa Y, Tsuji M, Kawaguchi A, Kohjiya S, Cakmak M. Polymer 1995;36(2):291.
[11] Cakmak M, Lee SW. Polymer 1995;36(21):4039.
[12] Kim JC, Cakmak M, Zhou X. Polymer 1998;39:4225.
[13] Cakmak M, Simhambhatla M. Polym Eng Sci 1995;35(9):1562.
[14] Ozisik R, Cakmak M. In: Proceedings, SPE, ANTEC, vol. 2; 1995. p. 1719.
[15] Statton WO, Godard GM. J Appl Phys 1957;28:1111.
[16] Bicakci S, Cakmak M. Polymer 1998;39(17):4001–10.
[17] Bicakci S, Cakmak M. Polymer 1998;39(22):5405–20.
[18] Bicakci S, Zhou X, Cakmak M. In: Proceedings, SPE ANTEC, vol. 2; 1997. p. 1600.
[19] Blundell DJ, Osborn BN. Polymer 1980;21:577.
[20] White JL, Spruiell JE. Polym Eng Sci 1981;21:850.
[21] Wilchinsky ZW. J Appl Phys 1959;30:792.
[22] Wilchinsky ZW. J Appl Phys 1960;31:1969.
[23] Wilchinsky ZW. J Appl Polym Sci 1963;7:923.
[24] Cakmak M, Lee SW. Polymer 1995;36:21.
[25] Buchner S, Wiswe D, Zachmann HG. Polymer 1989;30:408.
[26] Dawson PC, Blundell DJ. Polymer 1980;21:577.
[27] Kim JC, Cakmak M. In: Proceedings, SPE ANTEC, vol. 2; 1995. p. 1453.